European Journal of Cell Biology 104 (2025) 151516

Contents lists available at ScienceDirect

European Journal of Cell Biology

journal homepage: www.elsevier.com/locate/ejcb

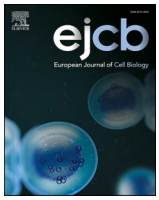

The cortical actin cytoskeleton and desmosomes act together in keratin filament network maintenance

Nicole Schwarz *, Sebastian Kant, Rudolf E. Leube *

Institute of Molecular and Cellular Anatomy, RWTH Aachen University, Wendlingweg 2, Aachen 52074, Germany

ARTICLE INFO

Keywords:
Keratin
Intermediate filaments
Embryogenesis
Actin
Desmosomes

ABSTRACT

Keratin intermediate filaments are hallmark features of epithelial tissue differentiation forming complex cytoplasmic networks that are connected to subplasmalemmal cortical keratin filaments and anchored at desmosomal junctions. The mechanisms determining keratin filament network morphogenesis and maintenance are poorly understood. We previously generated a homozygous knock-in mouse line expressing YFP-tagged keratin 8, which functionally substitutes for the wild-type keratin 8. 3D time-lapse fluorescence recording of developing preimplantation embryos allowed monitoring the de novo formation of the keratin filament network, which implicated desmosomes and the actin-rich cell cortex in nucleation and transport of nascent keratin particles. To further explore the relevance of the cell cortex for keratin filament network maintenance, we now studied Krt8-YFP-producing late blastocysts that had developed cytoplasmic and cortical keratin networks. We treated them with drugs to modulate the actomyosin cytoskeleton and analyzed desmosome-deficient blastocysts. We find that overall keratin network organization is barely affected in either scenario. Detailed analyses, however, reveal distinct changes in cytoplasmic keratin filament abundance, cortical anchorage and keratin filament turnover. We conclude that mature keratin networks withstand drastic changes in cellular organization and that maintenance of their spatial organization is secured in a "belt and braces" fashion by multiple mechanisms, notably desmosomal anchorage and attachment to the actin-rich cell cortex.

1. Introduction

Epithelial tissue properties are in large part determined by the cytoskeleton. It consists of different filament systems, each with unique biochemical, mechanical and dynamic features forming separate 3D networks with specialized functions (Lorenz and Köster, 2022; Pradeau-Phélut and Etienne-Manneville, 2024). How they are coordinated in space and time to support tissue homeostasis has been and continues to be a major research topic in epithelial cell biology (Bragulla and Homberger, 2009; Perrin and Matic Vignjevic, 2023; Outla et al., 2025). A hallmark of the epithelial cytoskeleton is the keratin intermediate filament network. It is composed of keratin polypeptides that are particularly abundant and diverse (Moll et al., 2008; Bragulla and Homberger, 2009; Jacob et al., 2018; Di Russo et al., 2023). Keratin filaments are attached to desmosomes at cell-cell borders and to hemidesmosomes at the epithelial-extracellular matrix interface (ECM) forming a transcellular scaffold that is firmly attached to the extracellular fiber systems (Hatzfeld et al., 2017; Laly et al., 2021; Di Russo et al., 2023). We have suggested that keratin filament network mechanics rely on a rim-and-spokes system, whereby subplasmalemmal cortical keratin filaments (the rim) are connected to radial keratin filaments (the spokes), which are linked to a perinuclear cage (Quinlan et al., 2017). Disruption of this system either within or at the junctional contacts results in tissue fragility giving rise to many genetic and acquired human diseases (Coulombe et al., 2009; Knöbel et al., 2015; Toivola et al., 2015). The underlying molecular mechanisms guiding and maintaining keratin filament network morphogenesis are poorly understood.

A major line of research has investigated the role of the actin cytoskeleton in keratin filament network organization (Celis et al., 1984; Kitajima et al., 1986; Wolf and Mullins, 1987; Gard et al., 1997; Wöll et al., 2005; Kölsch et al., 2009; Laly et al., 2021; Moch and Leube, 2021). These studies showed that interfering with actin polymerization impacts keratin filament network morphology and dynamics. The induced phenotypes, however, ranged from complete network collapse (Wöll et al., 2005) to keratin filament retraction (Windoffer and Leube, 1999; Kölsch et al., 2009) and various types of keratin filament remodeling such as keratin bundling (Moch and Leube, 2021) and

* Corresponding authors.
E-mail addresses: nschwarz@ukaachen.de (N. Schwarz), rleube@ukaachen.de (R.E. Leube).

https://doi.org/10.1016/j.ejcb.2025.151516
Received 5 June 2025; Received in revised form 8 August 2025; Accepted 4 September 2025
Available online 5 September 2025

keratin star formation (Celis et al., 1984; Kitajima et al., 1986; Wolf and Mullins, 1987; Gard et al., 1997). The reasons for these different responses have not been identified but cellular differentiation and keratin isotypes may be contributing factors. When interpreting the observed phenotypes, one must keep in mind that most investigations were carried out on single, transformed and rapidly proliferating cells. These non-physiological situations require a highly plastic cytoskeleton to adapt to the shape changes associated with cell motility, growth and division. The previous studies therefore focused on the influence of the dynamic actin system on the de novo formation and transport of keratin filaments. While actin does not affect keratin polymerization per se it is involved in the directed movement of nascent keratin filaments from the cell periphery towards the cell center (Wöll et al., 2005; Kölsch et al., 2009).

Much less is known about the consequences of modifying the actin system in normal tissues with a well-developed keratin network. To address this aspect, we decided to examine murine blastocysts. They are circumferentially covered by the placentogenic epithelial trophectoderm, encompass the embryogenic inner cell mass, are filled with fluid in their central blastocoelic cavity and are enveloped by the protective *zona pellucida*. The trophectoderm is the first tissue to develop a cytoplasmic intermediate filament network which is composed of the simple keratins 7, 8, 18 and 19 that are attached to desmosomes (Oshima et al., 1983; Chisholm and Houliston, 1987; Lu et al., 2005). We make use of Krt8-YFP knock-in mice that produce fluorescent keratin 8 from the endogenous keratin 8 gene locus (Schwarz et al., 2015). Distinct keratin granules can be observed at the cell borders of the blastomeres in eight-cell stage embryos. During morula formation the juxtamembranous keratin granules persist and colocalize with desmosomes. Subsequently they give rise to short cytoplasmic keratin filament precursors (Moch et al., 2020). After blastocyst formation, an interconnected mature keratin network develops in the trophectoderm spanning the entire cytoplasm and featuring the previously described rim-and-spokes arrangement (Quinlan et al., 2017). The morula-to-blastocyst transition is also marked by drastic changes in the actin cytoskeleton. While an actin-rich cell cortex is maintained throughout, conspicuous F-actin rings appear at the apical cortex of the outer cells of the 8-cell embryo (Zenker et al., 2018). These rings expand to cell-cell adhesions and lead to the sealing of the embryo. Interestingly, it has been suggested that intermediate filaments and actin filaments are together involved in cell fate specification during blastocyst formation (Lim et al., 2020; Lim and Plachta, 2021).

The current study aimed to find out how modulation of the actomyosin system and desmosomal anchorage affect the rim-and-spokes architecture of the matured keratin filament network in the murine trophectoderm.

2. Material and methods

2.1. Transgenic mice

Mice were housed in the animal facility of the RWTH Aachen University Hospital. All experiments were performed in accordance with the approved guidelines for the care and use of laboratory animals and reported to the Landesamt für Natur, Umwelt und Verbraucherschutz (LANUV) / Landesamt für Verbraucherschutz und Ernährung (LAVE), Nordrhein-Westfalen, Recklinghausen, Germany (reference numbers 11366A4 and 11492A4).

Krt8-YFP mice producing YFP-tagged keratin 8 have been described (Schwarz et al., 2015). For genotyping PCR primers #07–088 5'-AGG AGA GCA GGT GGG TTT GG-3' and #12–080 5'-CCC TCC CAC CTA CAC GAA TG-3' were used to amplify a 1100 bp fragment from the wild-type Krt8 allele and a 1871 bp fragment from the Krt8-YFP knock-in allele.

Desmoglein 2 knock-out mice have been characterized (Eshkind et al., 2002). For genotyping PCR primers #03–58 5'- AGGAAATGAAGGGGGCTATT-3', #03–59 5'-CTCTGAAAGGCAAGTAACTG-3' and #04–43 5'-CCCCGGATCTAAGCTCTAGATA-3' were used to amplify a 400 bp fragment from the wild-type desmoglein 2 allele and a 530 bp fragment from the mutated desmoglein 2 allele.

2.2. Pre-implantation embryo isolation

Pre-implantation embryos were isolated as described previously (Schwarz et al., 2016). In short, pre-implantation embryos were flushed out from oviducts of pregnant mice at day E2.5 with M2 medium (Sigma-Aldrich, Taufkirchen, Germany) and rinsed through several drops of fresh M2 medium to remove debris. They were kept in culture overnight in M16 medium (Sigma-Aldrich) at 37°C and 5 % CO_2. Only embryos that developed into blastocysts were used.

2.3. Inhibitor treatment

Blastocysts were identified by their extensive blastocoel, flattened trophectodermal cells and visible inner cell mass. Blastocysts were treated either with 100 nM jasplakinolide (Tocris Bioscience, Wiesbaden, Germany), 10 μM latrunculin B (Adipogen, Fuellinsdorf, Switzerland), 10 μM cytochalasin D (Sigma-Aldrich), 10 μM para-nitroblebbistatin (optopharma, Budapest, Hungary), 200 μM CK666 (Tocris Bioscience), 100 μM SMIFH2 (Tocris Bioscience) or dimethyl sulfoxide (DMSO) for 1 h. Incubation time and drug concentrations were optimized in living intestine of Krt8-YFP mice based on available literature. Blastocysts were either imaged during incubation or fixed afterwards for immunofluorescence staining.

2.4. Live cell imaging

Embryos were individually transferred into drops of M2 medium overlaid with mineral oil in glass-bottom dishes (MatTek). Images were recorded with a Zeiss LSM 710 Duo confocal microscope at 37°C using Zen black 2.1 SP3 software. The 488 nm line of an argon-ion laser (Laser module LGK 7872 ML8, Zeiss) at 0.4–1 % power was used for fluorescence recording via an oil immersion objective (63x/1.40-N.A. DIC M27). The z-resolution was set to 0.173 μm and the equipped AiryScan detector was used in super resolution mode. For transmitted light recordings the T-PMT detector of the microscope was used.

2.5. Fluorescence recovery after photobleaching

Embryos were individually transferred into drops of M2 medium overlaid with mineral oil in glass-bottom dishes (MatTek). Photobleaching experiments were performed with a Zeiss LSM 710 Duo confocal microscope equipped with a DefiniteFocus device (Zeiss) at 37°C. The 488 nm line of an argon-ion laser was used for both bleaching and image recording via a 63 × 1.4 N.A. DIC M27 oil immersion objective. The emitted light was monitored between 500 nm and 590 nm. Bleaching in selected areas was carried out at 100 % laser power for 2 scans with a pixel dwell time of 6.3 μs. The fluorescence intensity was measured at 1 % laser power in the respective areas of interest prior to bleaching and directly after bleaching at 30-second intervals for 15 min.

2.6. Immunofluorescence

Embryos were fixed with 1 % (w/v) paraformaldehyde (PFA) for 10 min at room temperature. Subsequently, embryos were transferred to 0.25 % (v/v) Triton X-100 in PBS for 15 min, washed with PBS for 15 min and incubated with 2.6 mg/ml ammonium chloride in PBS for 10 min. Embryos were then stored in PBS at 4°C until further use.

For staining, embryos were incubated over night at 4°C with primary antibodies (anti-actin: A2066, Sigma-Aldrich; anti-nmmIIa: 90801, BioLegend, San Diego, USA; anti-desmoplakin: DP-1, Progen, Heidelberg, Germany) diluted in PBS containing 2.5 % (w/v) bovine serum

albumin (BSA) and 0.125 % Triton X-100. After washing with PBS containing 0.25 % (v/v) Triton X-100 for 30 min at room temperature, embryos were incubated for 1 h at room temperature with appropriate secondary antibodies (anti-rabbit Alexa633-conjugated, A-21072, ThermoFisher; anti-guinea pig DyLight405-conjugated, 706–475–148, Dianova, Hamburg, Germany) diluted in PBS containing 2.5 % (w/v) bovine serum albumin (BSA) and 0.125 % (v/v) Triton X-100. Embryos were then washed with PBS for 30 min and either directly imaged or

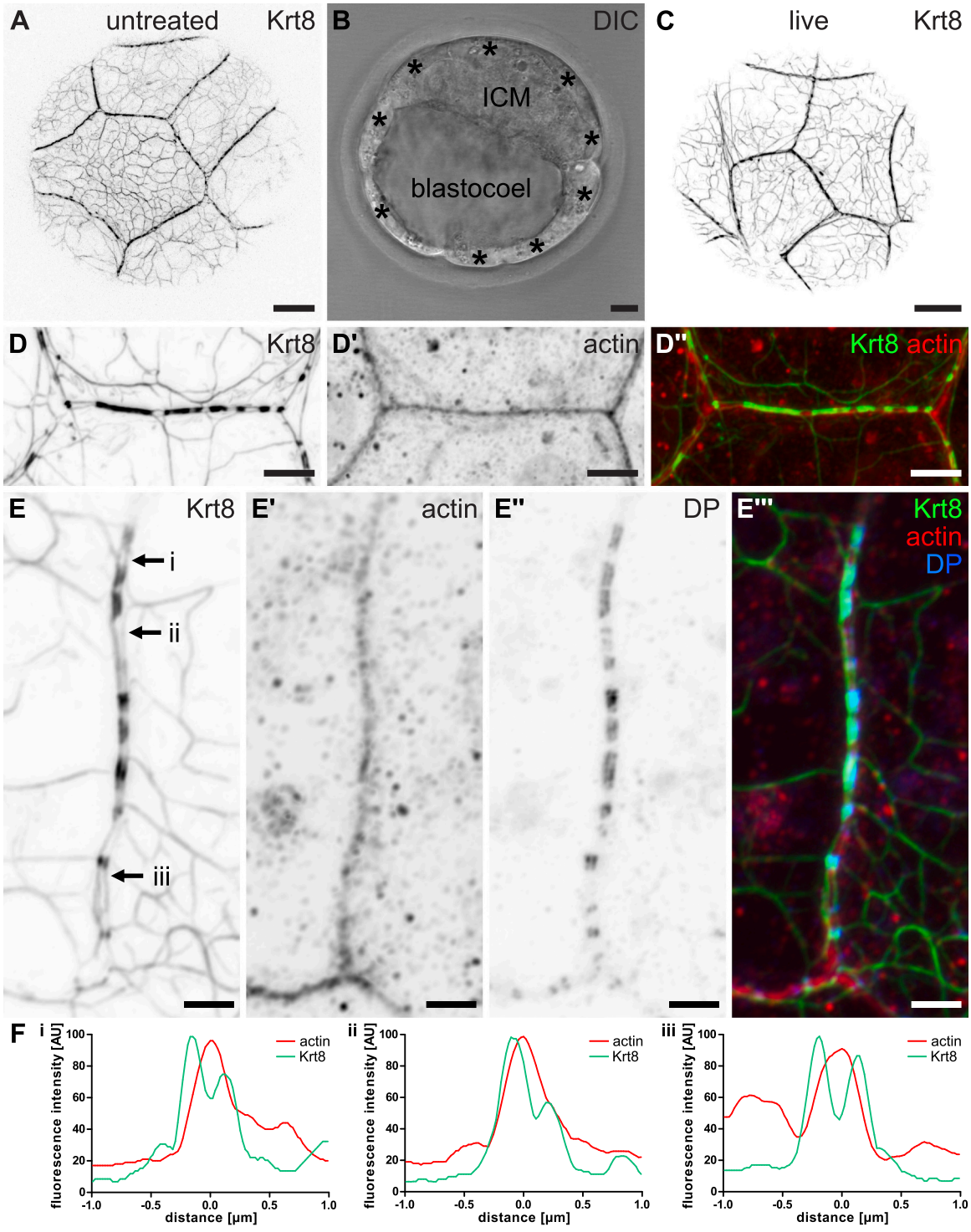

Fig. 1. A dense keratin filament network is positioned below the actin-rich cell cortex and is attached to desmosomes. The fluorescence micrographs depict the distribution of Krt8-YFP (inverse presentation) (A, C, D, E), actin (detected by antibodies in D', E') and desmoplakin (detected by antibodies in E''; merged images in D'', E''') in mid to late blastocysts (differential interference contrast (DIC) image in (B). Note that a pancytoplasmic keratin network can be detected in untreated and fixed (A), in DMSO treated and fixed (D) as well as living (C) samples. At the same time, pronounced keratin accumulations are seen at the plasma membrane which correspond to desmosomes (E, E'', E'''). They are connected by keratin filaments, which are subjacent to the actin cortex (D-D''). (F) Line plots of the indicated positions in (E) show the distribution of the fluorescence intensities of Krt8-YFP (green) and actin (red). Asterisks in (B) mark the trophectoderm. ICM = inner cell mass. AiryScan modus was used in (C-E'''). Maximum intensity projections are shown in (A, C-E'''). Scale bars in (A-C) = 10 µm and in (D-E''') = 2 µm.

stored at 4°C in PBS.

Imaging was done on free floating embryos in drops of M2 medium overlaid with mineral oil in glass-bottom dishes (MatTek) with a Zeiss LSM 710 Duo confocal microscope using an oil immersion objective (63x/1.40-N.A. DIC M27) and Zen black 2.1 SP3 software. For detection of Alexa633 fluorescence a 633 nm HeNe laser (Laser module LGK 7628–1 F, Zeiss) and for detection of DyLight405 fluorescence a diode laser (Laser cassette 405cw, Zeiss) were used. The 488 nm line of an argon-ion laser (Laser module LGK 7872 ML8, Zeiss) was used for recording of the Krt8-YFP fluorescence. The z-resolution was set to 0.173 μm and the AiryScan detector was used in super resolution mode in some instances. For transmitted light recordings the T-PMT detector of the microscope was used.

2.7. Image analysis and statistics

Microscopy images were processed and analyzed using Fiji (ImageJ). Statistical testing was done in Prism 5 (GraphPad).

For measurements of dense spots per 100 μm membrane length measurements Fiji was used to determine the plasma membrane length and the number of dense spots along this membrane. All membranes that were in focus of each blastocyst were analyzed. Data are given as mean + /- SD and significance of differences was tested using a one-way analysis of variance and subsequent Bonferroni's multiple comparison test.

For FRAP analysis the gray values of the bleached and reference areas were measured in the recorded image data sets. Data are given as mean + /- SD and significance of differences was tested using a one-way analysis of variance and subsequent Bonferroni's multiple comparison test.

3. Results

3.1. The cortical keratin network is in direct apposition to the actin-rich cell cortex and is enriched at desmosomes

We have previously shown that the keratin intermediate filament network forms to its full extent during the mid to late blastocyst stage (Schwarz et al., 2015). At this time a distinct architecture can be discerned consisting of a cytoplasm-spanning 3D scaffold and juxtamembraneous cortical keratin filaments. It is restricted to the trophectoderm that surrounds the blastocoel and inner cell mass (Fig. 1A-C). This architecture is preserved after fixation (Fig. 1A, C). The cortical portion of the keratin network can be subdivided into keratin accumulations at desmosomes and inter-desmosomal keratin filament bundles (Fig. 1D). It has been shown that the cortical keratin filament network is positioned immediately below the actin cortex in different cell types, tissues and organisms (Hirokawa and Heuser, 1981; Grimm-Günter et al., 2009; Coch and Leube, 2016; Quinlan et al., 2017; Tateishi et al., 2017; Geisler et al., 2020). To find out whether this is also the case in the trophectoderm, we co-localized actin and keratin (Fig. 1D-D''). High magnification imaging identified two distinct layers of keratin filaments each of which is underneath the plasma membranes of adjacent cells with interspersed desmosomes and actin located between the keratin layers (Fig. 1D-F). This arrangement suggests that both filament systems are in direct contact and may influence the distribution of each other and their anchorage to the plasma membrane.

3.2. Stabilization of filamentous actin leads to drastic shape changes of the trophectoderm with only minor effects on overall keratin network organization

To study the role of actin filament dynamics for keratin network organization, we treated embryos with jasplakinolide. Jasplakinolide reduces actin filament turnover and increases actin polymerization (Bubb et al., 1994). The blastocoel of the treated blastocysts collapsed within 1 h. The once flat trophectoderm cells became cuboidal (compare Fig. 2A' with 1B). Yet, the treatment did not alter the overall architecture of the keratin filament network. The cortical and cytoplasmic keratin filament networks were still present (Fig. 2A, C). Nevertheless, the cytoplasmic network was less developed than in the untreated or DMSO-treated controls (compare Fig. 2A, B with Fig. 1A, D). The filaments were thinner and more diffuse cytoplasmic fluorescence was detectable.

3.3. Inhibition of actin filament polymerization enhances and alters the cortical keratin network

In the next set of experiments, we wanted to examine the effect of preventing actin polymerization on keratin network organization. To this end, we used cytochalasin D and latrunculin B both of which interfere with actin polymerization but function differently. Cytochalasin D occupies the barbed plus end of F-actin preventing the attachment of actin monomers while latrunculin B binds to actin monomers preventing them from attaching to the barbed ends of F-actin (Spector et al., 1989). Both actin inhibitors induced a rearrangement of the keratin intermediate filament network. The cytoplasmic keratin filament network was considerably reduced after 1 h of treatment. The effect was more pronounced for latrunculin B than for cytochalasin D (compare Fig. 3A and Fig. 3E). At the same time, the cortical keratin fluorescence was visibly broadened (Fig. 3A, B, E, F). While prominent cortical keratin accumulations remained, we observed an increase in the distance between the cortical keratin networks of adjacent cells in drug-treated blastocysts (compare Fig. 1D, E with Fig. 3B, F). This change went along with a tortuous distribution of the cortical keratins. Together, these observations suggest that the interdesmosomal, cortical keratin filaments lose their tight membrane association in the absence of a functional actin cortex. Another conspicuous observation was that most of the forming actin accumulations remained in close apposition to keratins (Fig. 3C, D, G, H). This can be taken as an indication of either intrinsic affinity or molecular linkage between actin and keratin.

3.4. Inhibition of actin filament nucleation has no major short-term effect on keratin filament network organization

We next interfered with actin filament nucleation, which is regulated by formins and the Arp2/3 complex. Formins possess a conserved FH2 domain that dimerizes to nucleate and elongate straight actin filaments (Pruyne et al., 2002). The Arp2/3 complex creates branch points of actin filaments where it stimulates actin assembly resulting in a branched network (Mullins et al., 1998). One hour incubation of blastocysts with the formin FH2 domain inhibitor SMIFH2 did not induce visible changes in the overall structure of the embryo or the keratin intermediate filament network (Fig. 4A-B). On the other hand, treatment with the Arp2/3 inhibitor CK666 for 1 h led to a collapse of the blastocysts with a reduced blastocoel (Fig. 4C'). Although the trophectodermal cells acquired a rounded shape the cortical and cytoplasmic keratin networks remained (Fig. 4C-D). High-resolution imaging of tricellular junctions indicated a slightly reduced coherence. Conspicuous keratin filaments bridging the contact regions were reduced in the SMIFH2-treated embryos (Fig. 4E-G).

3.5. Inhibition of myosin leads to wrinkling of the plasma membrane and the associated cortical keratins

To test whether and how membrane tension affects the cortical keratin network organization we treated blastocysts with para-nitro-blebbistatin. Para-nitro-blebbistatin is a photostable, non-cytotoxic alternative to blebbistatin, which inhibits non-muscle myosin II and therefore leads to relaxation of the acto-myosin system (Képiró et al., 2014). The trophectodermal plasma membranes became wrinkled after a 1-hour treatment with para-nitro-blebbistatin (Fig. 5). The cortical

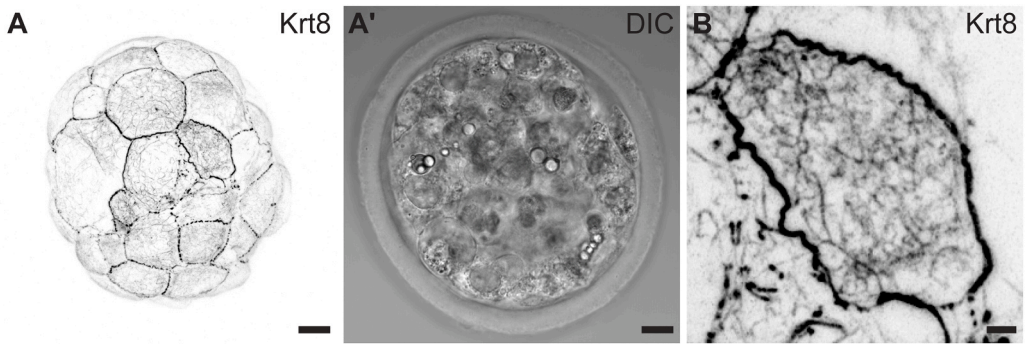

Fig. 2. Jasplakinolide-induced actin filament stabilization leads to collapse of the blastocoel and trophectodermal shape changes with only minor impact on cortical and cytoplasmic keratin filament localization. The fluorescence image in (A) shows the distribution of Krt8-YFP (inverse presentation) with the corresponding brightfield in (A') (differential interference contrast, DIC) of a blastocyst that had been treated with 100 nM jasplakinolide for 1 h. Note the collapse of the blastocoel and the rounding of the trophectodermal cells. The overall architecture of the keratin network is not changed. The magnification in (B) shows an image with increased exposure to highlight the slightly increased diffuse cytoplasmic fluorescence and the reduced cytoplasmic keratin network with thin fibers and a smaller mesh size. n = 3 blastocysts. AiryScan modus was used in (B). Maximum intensity projections are shown in (A, B). Scale bars in (A-A') = 10 μm and in (B) = 2 μm.

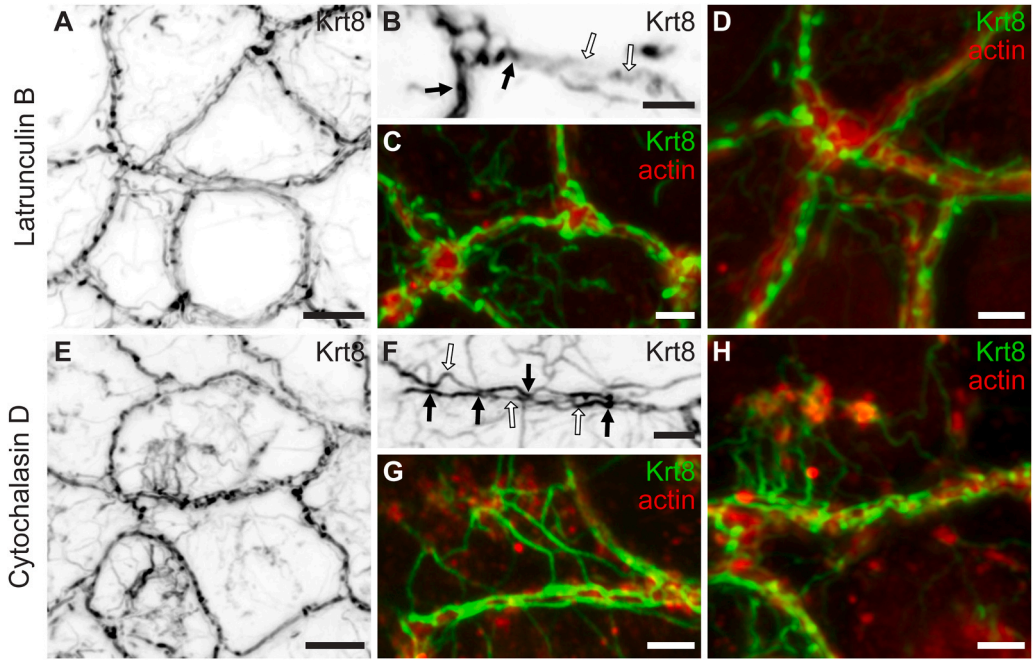

Fig. 3. Cytochalasin D and latrunculin B induce a reduction of keratin filaments in the cytoplasm and enrichment in the cell cortex, albeit with increased distance to the plasma membrane. The fluorescence micrographs show the distribution of Krt8-YFP alone (inverse presentation) (A, B, E, F) or together with actin (detected by antibodies in red) (C, D, G, H) in blastocysts after treatment with either 10 μM latrunculin B or 10 μM cytochalasin D for 1 h. Note the reduction of the cytoplasmic keratin network, which is almost completely absent in the latrunculin-treated trophoblast. At the same time, cortical keratin fluorescence is increased (B, F) while cortical actin is drastically reduced and cytoplasmic actin aggregates are formed (C, D, G, H). In several instances, keratin decorates the actin accumulations (H). The cortical keratin shows a large gap between adjacent cells (white arrows) while retaining the juxtamembraneous accumulations (black arrows). Note also the tortuous component of the cortical keratin. n = 5–6 blastocysts. AiryScan modus was used in (A-H). Maximum intensity projections are shown in (A-H). Scale bars in (A, E) = 5 μm and in (B-D, F-H) = 2 μm.

keratin filaments mirrored these changes but did not become separated as was the case for cytochalasin D- and latrunculin B-treated blastocysts. Since the wrinkling was accompanied by a slight increase of the overall keratin rim length (~7.6 %), we conclude that the keratin filaments remained attached to the cell cortex. The overall architecture of the cytoplasmic keratin network appeared to be unaffected.

3.6. Loss of desmoglein 2 leads to reduced keratin accumulations at cell borders

To figure out the contribution of desmosomes to the cortical keratin localization we crossed Krt8-YFP mice (Schwarz et al., 2015) with desmoglein 2 knock-out mice (Eshkind et al., 2002). The cytoplasmic keratin network in the trophectoderm of the different genotypes did not show major differences in early blastocysts (Fig. 6 A-C'). The number of cortical granular keratin accumulations, however, was strongly reduced in the desmoglein 2 mutant background resulting in a more even distribution of the cortical keratin fluorescence (Fig. 6B-D). To find out whether properties of the keratin granule-depleted cortical cytoskeleton was altered, we performed fluorescence recovery after photobleaching experiments. They revealed that the keratin filament turnover was reduced in heterozygous and homozygous desmoglein 2 knock-out blastocysts (Fig. 6E). We take this as an indication that the cortical, non-desmosomal keratin filaments are more stable than the desmosomal

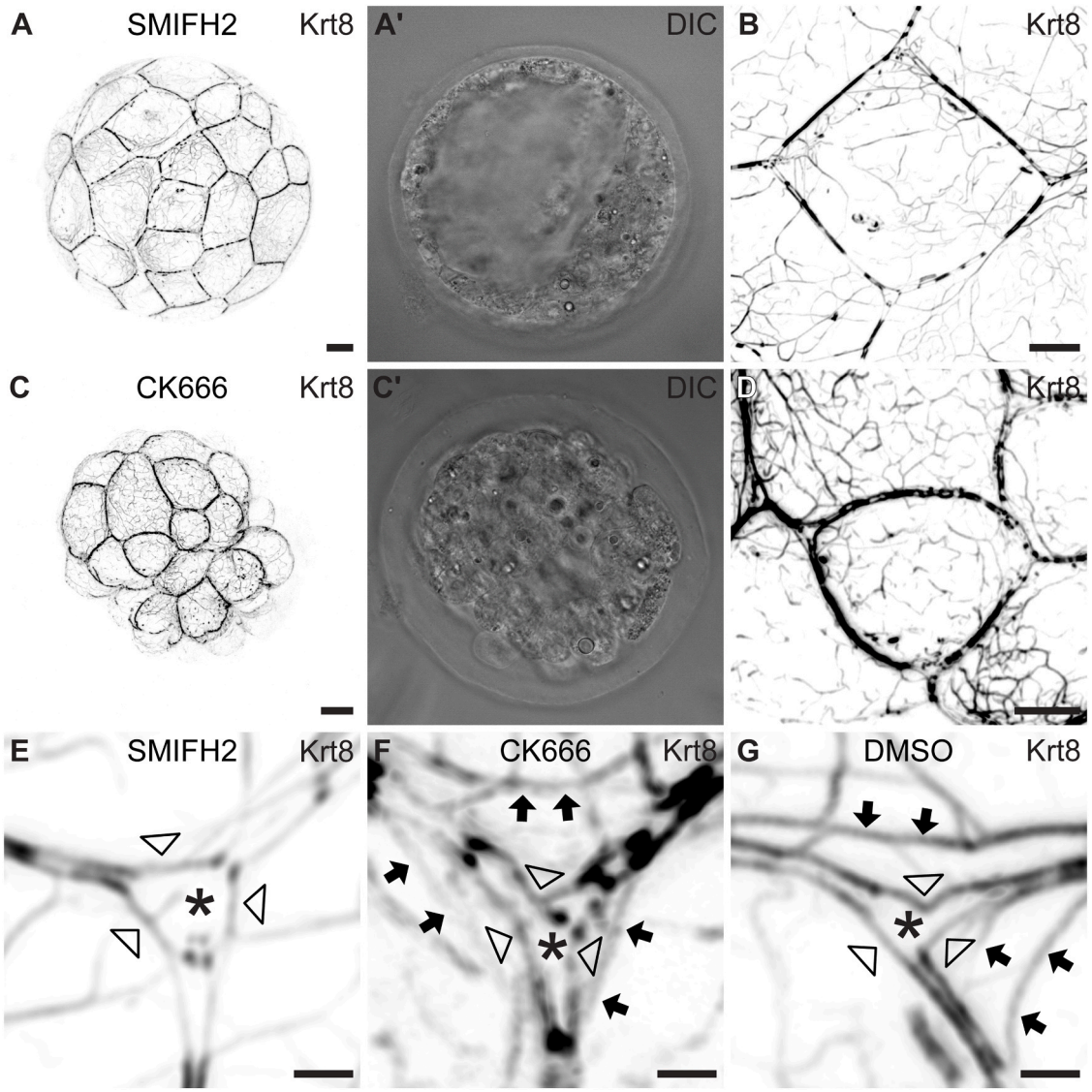

Fig. 4. The formin inhibitor SMIFH2 induces no obvious alterations in blastocyst morphology whereas the Arp2/3 inhibitor CK666 induces blastocyst collapse. Keratin network organization is, for the most part, maintained.The microscopic images show Krt8-YFP fluorescence in inverse presentation (A, B, C, D, E, F, G) and corresponding brightfield pictures (A', C') that were recorded in blastocysts after treatment with either 100 μM SMIFH2 or 200 μM CK666 for 1 h. No obvious changes in the morphology and keratin network organization are visible in the SMIFH2-treated blastocysts whereas in the CK666-treated blastocysts a blastocoel collapse and trophectodermal cell rounding are observed. The high magnification images in (E-G) illustrate the reduced coherence of tricellular junctions in the drug-treated samples. Asterisks demarcate the position of tricellular junctions, open arrowheads depict the cortical keratin signals, and the arrows point to bridging keratin filaments. n = 3 blastocysts. AiryScan modus was used in (A-G). Maximum intensity projections are shown in (A-G). Scale bars in (A-A' and B-B') = 10 μm, in (B, D) = 5 μm and in (E, F, G) = 1 μm.

keratin accumulations.

4. Discussion

The keratin intermediate filament network in trophectodermal cells of the blastocyst is organized in accordance with the previously described rim-and-spokes architecture consisting of a cortical network that interconnects desmosomes and a radial cytoplasmic network (Quinlan et al., 2017). The cell cortex is formed by a dense layer of actin filaments and actin-binding proteins underneath the plasma membrane (Fritzsche et al., 2013). As this actin cortex is in close proximity with the cortical keratin system it has been suggested that keratins interact with the actomyosin cytoskeleton in epithelial cells either directly or indirectly. Thus, intimate contact between actin and keratin has been reported in the past in different contexts (Hirokawa et al., 1982; Green et al., 1987; Gard et al., 1997; Toivola et al., 1997). In vitro experiments further showed that mixed actin-keratin filament systems exhibit unique mechanical properties (Elbalasy et al., 2021). Recent in silico analyses provide evidence that coil 2 of several keratins may bind directly to actin (Schwarz et al., 2025). On the other hand, plectin has been identified as a major linker between both filament systems (Bouameur et al., 2014; Outla et al., 2025). This connectivity has been shown to be of relevance for cellular tension and cohesion in epithelial monolayers (Prechova et al., 2022). Another linker is plastin 1, which plays a major role in linking the subapical keratin cytoskeleton of intestinal cells to the actin-rich terminal web region (Grimm-Günter et al., 2009). Finally, myosin motors have been implicated in coupling actin and keratin (Kwan et al., 2015; Wang et al., 2018; Lehmann et al., 2021). We do not know which mechanisms are relevant in the blastocyst but the keratin network must act together with actin in the trophectoderm to provide the mechanical resilience to withstand the forces from the pressurized blastocoel (Chan et al., 2019).

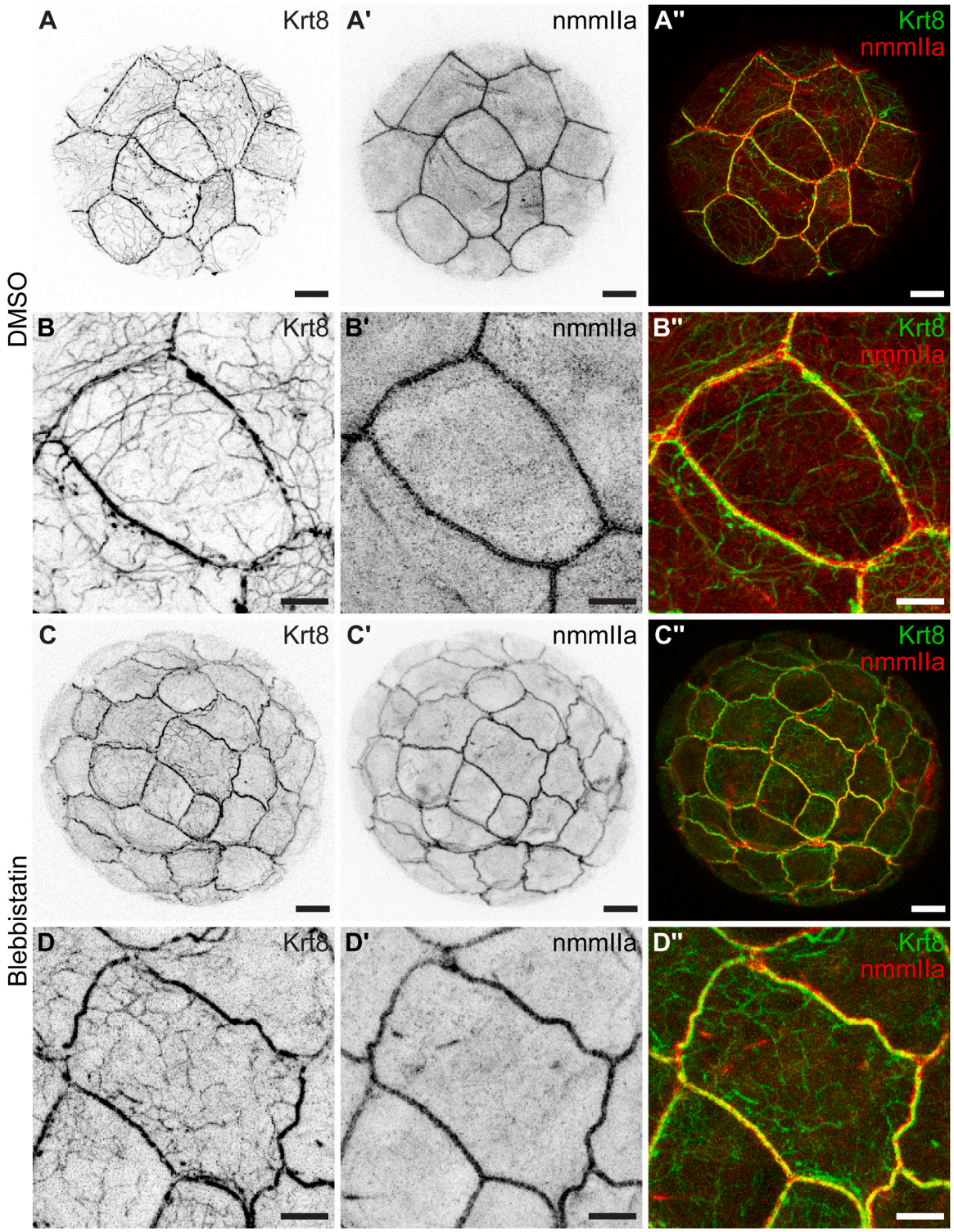

Fig. 5. Inhibition of actomyosin-dependent tension leads to wrinkling of the cortical keratin network. The fluorescence micrographs show the distribution of Krt8-YFP (inverse presentation) (A, B, C, D) and anti-non-muscle myosin IIa (nmmIIa) immunoreactivities (inverse presentation) (A', B', C', D'; merged color images in A'', B'', C'', D'') in blastocysts treated for 1 h either with the DMSO solvent alone (A-B'') or 10 μM para-nitro-blebbistatin (C-D''). Note that both the cortical nmmIIa and keratin fluorescence remain co-localized but become tortuous reflecting the reduced cortical tension in the drug treated blastocysts. The cytoplasmic keratin network is not affected. n = 5–7 blastocysts. AiryScan modus was used in (A-D''). Maximum intensity projections are shown in (A-D''). Scale bars in (A-A'' and C-C'') = 10 μm and in (B-B'' and D-D'') = 5 μm.

Previous studies have mostly focused on functions of the actin filament system during early embryogenesis. Treatment of pre-implantation embryos with the actin filament stabilizing jasplakinolide led to an arrest of early embryo development and prevented apical domain formation in 8-cell stage embryos (Rawe et al., 2006; Zhu et al., 2020). Interestingly, it was also reported that jasplakinolide treatment causes contractions of late bovine blastocysts (Yamamura et al., 2020). The shape changes of the trophectodermal cells and the overall collapse of

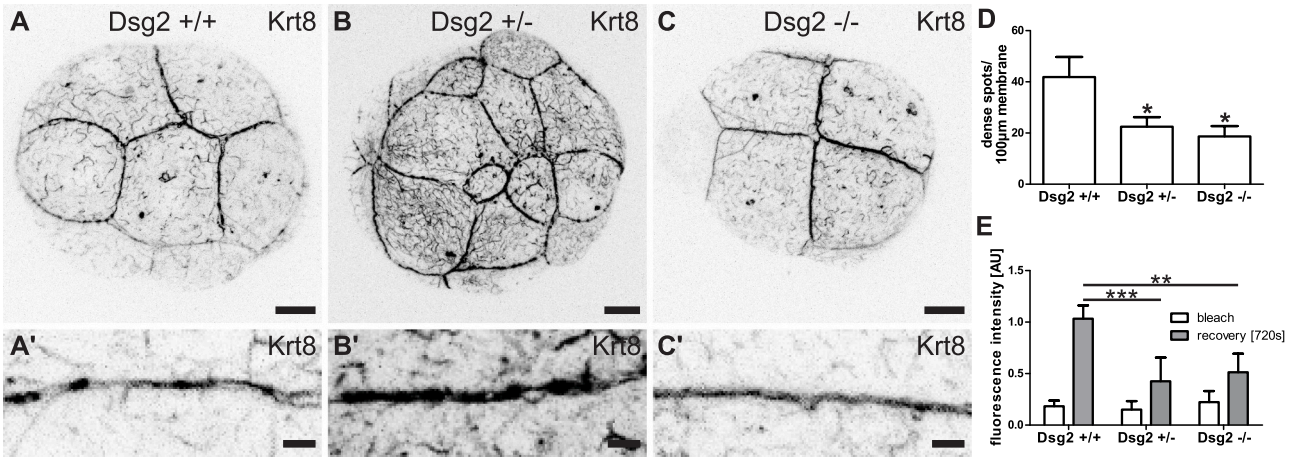

Fig. 6. Desmosome reduction decreases the turnover of the cortical keratin network. The fluorescence micrographs reveal the distribution of Krt8-YFP in a wild-type blastocyst ($Dsg2^{+/+}$) (A-A'), a heterozygous ($Dsg2^{+/-}$) (B-B') and a homozygous ($Dsg2^{-/-}$) desmoglein 2-knockout blastocyst (C-C'). Note the presence of cytoplasmic and cortical keratin filaments in the heterozygous and homozygous knockout blastocysts, which, however, lack the characteristic multipunctate cortical Krt8-YFP pattern (B'-C'). The histogram shows the results of determining the dense cortical keratin accumulations in wild-type ($Dsg2^{+/+}$), heterozygous ($Dsg2^{+/-}$) and homozygous knockout blastocysts ($Dsg2^{-/-}$) per 100 µm membrane length (D). n = 7–14 blastocysts, *$p < 0.05$ (E) The histogram depicts the results of fluorescence recovery after photobleaching experiments revealing that the turnover of the membranous Krt8-eYFP signal is significantly reduced in heterozygous and homozygous Dsg2-knockout blastocysts. n = 3–12 blastocysts, **$p < 0.01$, ***$p < 0.001$. Maximum intensity projections are shown in (A-C'). Scale bars in (A-C) = 10 µm and in (A'-C') = 2 µm.

the blastocyst were not reported before but fit the already described loss of polarization. Along with the morphological changes, jasplakinolide induced diffuse cytoplasmic keratin fluorescence, likely reflecting an increase of the soluble keratin pool. These observations suggest that slow, long-term processes may have been initiated through the stabilization of the actin cytoskeleton, which impede keratin filament assembly and, conversely, favor cytoplasmic keratin filament disassembly. One should keep in mind that keratin turnover is comparatively slow with a half-life in the range of 30 minutes to several hours (Yoon et al., 2001; Kölsch et al., 2010; Moch et al., 2013; Schwarz et al., 2015).

It was further shown that inhibition of actin polymerization by cytochalasin D or B during the morula-to-blastocyst transition arrests development (Granholm and Brenner, 1976; Cheon et al., 1999). It was furthermore reported that treatment of blastocysts with latrunculin A or cytochalasin B for 4–8 hours leads to a collapse of the blastocyst cavity (Marikawa and Alarcon, 2018). This contrasts with our current study in which we did not observe this collapse. It may be due to the much shorter incubation period in our study at a slightly later developmental stage. Nevertheless, we were still able to detect distinct changes in keratin network organization under these comparatively mild conditions. The cortical keratin network was visibly enlarged. Given the observation that cortical tension in flattening trophectodermal cells increases during blastocyst maturation (Chan et al., 2019), the cortical keratin enrichment may reflect the redistribution of the cytoplasmic keratin network towards the site of highest tension after its release from filamentous actin (Latorre et al., 2018). This would explain why the disruption of actin polymerization by cytochalasin D in non-confluent cultured epithelial cells which lack cell-cell contacts typically leads to a seemingly contradictory effect, namely a collapse of the keratin network toward the nucleus (Wöll et al., 2005).

Actin filament formation is nucleated in two distinct ways: branching via the Arp2/3 complex and elongation by formins (Campellone and Welch, 2010). We show that the inhibition of the formin FH domains with SMIFH2 does not influence the morphology of the blastocyst nor the trophectodermal keratin network architecture. Treatment of blastocysts with the Arp2/3 inhibitor CK666, on the other hand, led to a collapse of the blastocoel and a rounded shape transformation of the trophectoderm. The Arp2/3 complex has previously been shown to be essential for early blastocyst development in part due to compromised apical-basal polarity (Sun et al., 2013). Apical-basal polarization begins in late 8 cell stage embryos and progresses during subsequent cell divisions when outer and inner cells appear. Outer cells, the future trophectoderm, retain their polarity markers, and start to form cell-cell junctions such as adherens junctions and desmosomes (Alarcon and Marikawa, 2022). Knock-out of E-cadherin, a component of adherens junctions, leads to a cuboidal trophectoderm without affecting desmosome or keratin localization (Ohsugi et al., 1997). Desmosomal cadherin Dsg2 knockout in blastocysts did not induce major morphological changes, and the cytoplasmic keratin network appeared to be unaffected for the most part. The prominent keratin accumulations at the plasma membrane, however, were diminished. This is in line with our previous observations that in the absence of Dsg2 very little desmoplakin is concentrated at cell membranes but is instead evenly distributed throughout the cell (Eshkind et al., 2002).

Non-muscle myosin II is located at the cell cortex in blastocysts and increases the tension at the junctions (Slager et al., 1992; Zenker et al., 2018). Inhibition of non-muscle myosin II with blebbistatin relaxes the membrane while keeping the blastocyst morphology. The result is the appearance of a curvy cell-cell interface as has been reported (Hildebrand et al., 2017). The cortical keratin follows this relaxation and also becomes curvy. These observations show that cortical keratin localization is not dependent on plasma membrane tension.

While we were able to detect distinct changes in keratin network organization in the trophectoderm of mid to late blastocysts in response to modulation of the actin system, we would like to emphasize that overall network morphology was surprisingly stable. This observation points to the resilience of the network once it is established and indicates that multiple mechanisms are at work to ensure its fail-safe damage tolerance. In the case of the cortical keratin network its stability appears to be secured by a robust "belt-and braces" system. It is safeguarded by linkage (i) to the cortical actin layer either directly or through linker molecules such as plectin and plastin 1 ("belt") and (ii) to desmosomes through linker molecules such as desmoplakin ("braces"). Tinkering with either cortical actin or desmosomes alone is therefore not sufficient to disrupt cortical keratin network localization. The observation that the distance of cortical keratin filaments to the plasma membrane was increased in cells treated with cytochalasin or latrunculin, however, indicates a partial dissociation. These observations also strongly argue against a direct keratin-lipid interaction as has been observed in other paradigms (Heid et al., 2013; Kuburich et al., 2024). It will be interesting

to see, how the release of cortical keratin filaments affects the mechanical properties of the cell cortex. Conversely, interfering with desmosomal anchorage through desmosome depletion in desmoglein 2 knockout embryos retained keratin filaments in the cell cortex but reduced their turnover. The latter may indicate an important function of desmosomes for cortical intermediate filament network remodeling as has been observed during desmosome formation (Moch et al., 2020). Further experiments are needed to determine whether cortical actin and desmosomes act alone or in combination with additional components in the regulation of the cortical keratin filament system.

CRediT authorship contribution statement

Rudolf E. Leube: Writing – review & editing, Validation, Funding acquisition, Conceptualization. **Nicole Schwarz:** Writing – review & editing, Writing – original draft, Visualization, Validation, Investigation, Formal analysis, Conceptualization. **Sebastian Kant:** Writing – review & editing, Validation, Resources.

Declaration of Competing Interest

The authors declare that they have no known competing financial interests or personal relationships that could have appeared to influence the work reported in this paper.

Acknowledgments

This work was supported by the German Research Council (DFG) (LE 566/20–1 and 363055819/GRK2415). The authors thank Nadine Böttcher for technical support. We also thank one of the Reviewers for suggesting the term “belt and braces” to convey our idea of safeguard redundancy of the cortical keratin network.

Data availability

Data will be made available on request.

References

Alarcon, V.B., Marikawa, Y., 2022. Trophectoderm formation: regulation of morphogenesis and gene expressions by RHO, ROCK, cell polarity, and HIPPO signaling. Reprod. Camb. Engl. 164, R75–R86. https://doi.org/10.1530/REP-21-0478.

Bouameur, J.-E., Favre, B., Borradori, L., 2014. Plakins, a versatile family of cytolinkers: roles in skin integrity and in human diseases. J. Invest. Dermatol. 134, 885–894. https://doi.org/10.1038/jid.2013.498.

Bragulla, H.H., Homberger, D.G., 2009. Structure and functions of keratin proteins in simple, stratified, keratinized and cornified epithelia. J. Anat. 214, 516–559. https://doi.org/10.1111/j.1469-7580.2009.01066.x.

Bubb, M.R., Senderowicz, A.M., Sausville, E.A., Duncan, K.L., Korn, E.D., 1994. Jasplakinolide, a cytotoxic natural product, induces actin polymerization and competitively inhibits the binding of phalloidin to F-actin. J. Biol. Chem. 269, 14869–14871. https://doi.org/10.1016/S0021-9258(17)36545-6.

Campellone, K.G., Welch, M.D., 2010. A nucleator arms race: cellular control of actin assembly. Nat. Rev. Mol. Cell Biol. 11, 237–251. https://doi.org/10.1038/nrm2867.

Celis, J.E., Small, J.V., Larsen, P.M., Fey, S.J., De Mey, J., Celis, A., 1984. Intermediate filaments in monkey kidney TC7 cells: focal centers and interrelationship with other cytoskeletal systems. Proc. Natl. Acad. Sci. 81, 1117–1121. https://doi.org/10.1073/pnas.81.4.1117.

Chan, C.J., Costanzo, M., Ruiz-Herrero, T., Mönke, G., Petrie, R.J., Bergert, M., Diz-Muñoz, A., Mahadevan, L., Hiiragi, T., 2019. Hydraulic control of mammalian embryo size and cell fate. Nature 571, 112–116. https://doi.org/10.1038/s41586-019-1309-x.

Cheon, Y.P., Gye, M.C., Kim, C., Kang, B.M., Chang, Y.S., Kim, S.R., Kim, M.K., 1999. Role of actin filaments in the hatching process of mouse blastocyst. Zygote 7, 123–129. https://doi.org/10.1017/S0967199499000477.

Chisholm, J.C., Houliston, E., 1987. Cytokeratin filament assembly in the preimplantation mouse embryo. Development 101, 565–582.

Coch, R.A., Leube, R.E., 2016. Intermediate filaments and polarization in the intestinal epithelium. Cells 5, 32. https://doi.org/10.3390/cells5030032.

Coulombe, P.A., Kerns, M.L., Fuchs, E., 2009. Epidermolysis bullosa simplex: a paradigm for disorders of tissue fragility. J. Clin. Invest 119, 1784–1793. https://doi.org/10.1172/JCI38177.

Di Russo, J., Magin, T.M., Leube, R.E., 2023. A keratin code defines the textile nature of epithelial tissue architecture. Curr. Opin. Cell Biol. 85, 102236. https://doi.org/10.1016/j.ceb.2023.102236.

Elbalasy, I., Mollenkopf, P., Tutmarc, C., Herrmann, H., Schnauß, J., 2021. Keratins determine network stress responsiveness in reconstituted actin-keratin filament systems. Soft Matter 17, 3954–3962. https://doi.org/10.1039/d0sm02261f.

Eshkind, L., Tian, Q., Schmidt, A., Franke, W.W., Windoffer, R., Leube, R.E., 2002. Loss of desmoglein 2 suggests essential functions for early embryonic development and proliferation of embryonal stem cells. Eur. J. Cell Biol. 81, 592–598. https://doi.org/10.1078/0171-9335-00278.

Fritzsche, M., Lewalle, A., Duke, T., Kruse, K., Charras, G., 2013. Analysis of turnover dynamics of the submembranous actin cortex. Mol. Biol. Cell 24, 757–767. https://doi.org/10.1091/mbc.E12-06-0485.

Gard, D.L., Cha, B.J., King, E., 1997. The organization and Animal–Vegetal asymmetry of cytokeratin filaments in stage VIXenopusOocytes is dependent upon F-Actin and microtubules. Dev. Biol. 184, 95–114. https://doi.org/10.1006/dbio.1997.8508.

Geisler, F., Coch, R.A., Richardson, C., Goldberg, M., Bevilacqua, C., Prevedel, R., Leube, R.E., 2020. Intestinal intermediate filament polypeptides in C. Elegans: common and isotype-specific contributions to intestinal ultrastructure and function. Sci. Rep. 10, 3142. https://doi.org/10.1038/s41598-020-59791-w.

Granholm, N.H., Brenner, G.M., 1976. Effects of cytochalasin b (CB) on the morula-to-blastocyst transformation and trophoblast outgrowth in the early mouse embryo. Exp. Cell Res. 101, 143–153. https://doi.org/10.1016/0014-4827(76)90423-7.

Green, K.J., Geiger, B., Jones, J.C., Talian, J.C., Goldman, R.D., 1987. The relationship between intermediate filaments and microfilaments before and during the formation of desmosomes and adherens-type junctions in mouse epidermal keratinocytes. J. Cell Biol. 104, 1389–1402. https://doi.org/10.1083/jcb.104.5.1389.

Grimm-Günter, E.-M.S., Revenu, C., Ramos, S., Hurbain, I., Smyth, N., Ferrary, E., Louvard, D., Robine, S., Rivero, F., 2009. Plastin 1 binds to keratin and is required for terminal web assembly in the intestinal epithelium. Mol. Biol. Cell 20, 2549–2562. https://doi.org/10.1091/mbc.e08-10-1030.

Hatzfeld, M., Keil, R., Magin, T.M., 2017. Desmosomes and intermediate filaments: their consequences for tissue mechanics. Cold Spring Harb. Perspect. Biol. 9, a029157. https://doi.org/10.1101/cshperspect.a029157.

Heid, H., Rickelt, S., Zimbelmann, R., Winter, S., Schumacher, H., Dörflinger, Y., 2013. Lipid droplets, perilipins and cytokeratins – unravelled liaisons in Epithelium-Derived cells. Plos ONE, 8, e63061. https://doi.org/10.1371/journal.pone.0063061.

Hildebrand, S., Hultin, S., Subramani, A., Petropoulos, S., Zhang, Y., Cao, X., Mpindi, J., Kalloniemi, O., Johansson, S., Majumdar, A., Lanner, F., Holmgren, L., 2017. The E-cadherin/AmotL2 complex organizes actin filaments required for epithelial hexagonal packing and blastocyst hatching. Sci. Rep. 7, 9540. https://doi.org/10.1038/s41598-017-10102-w.

Hirokawa, N., Heuser, J.E., 1981. Quick-freeze, deep-etch visualization of the cytoskeleton beneath surface differentiations of intestinal epithelial cells. J. Cell Biol. 91, 399–409. https://doi.org/10.1083/jcb.91.2.399.

Hirokawa, N., Tilney, L.G., Fujiwara, K., Heuser, J.E., 1982. Organization of actin, myosin, and intermediate filaments in the brush border of intestinal epithelial cells. J. Cell Biol. 94, 425–443. https://doi.org/10.1083/jcb.94.2.425.

Jacob, J.T., Coulombe, P.A., Kwan, R., Omary, M.B., 2018. Types I and II keratin intermediate filaments. Cold Spring Harb. Perspect. Biol. 10. https://doi.org/10.1101/cshperspect.a018275.

Képiró, M., Várkuti, B.H., Végner, L., Vörös, G., Hegyi, G., Varga, M., Málnási-Csizmadia, A., 2014. para-Nitroblebbistatin, the Non-Cytotoxic and photostable myosin II inhibitor. Angew. Chem. Int. Ed. 53, 8211–8215. https://doi.org/10.1002/anie.201403540.

Kitajima, Y., Inoue, S., Yaoita, H., 1986. Reorganization of keratin intermediate filaments by the drug-induced disruption of microfilaments in cultured human keratinocytes. J. Invest. Dermatol. 87, 565–569. https://doi.org/10.1111/1523-1747.ep12455792.

Knöbel, M., O'Toole, E.A., Smith, F.J.D., 2015. Keratins and skin disease. Cell Tissue Res 1–7. https://doi.org/10.1007/s00441-014-2105-4.

Kölsch, A., Windoffer, R., Leube, R.E., 2009. Actin-dependent dynamics of keratin filament precursors. Cell Motil. Cytoskelet. 66, 976–985. https://doi.org/10.1002/cm.20395.

Kölsch, A., Windoffer, R., Würflinger, T., Aach, T., Leube, R.E., 2010. The keratin-filament cycle of assembly and disassembly. J. Cell Sci. 123, 2266–2272. https://doi.org/10.1242/jcs.068080.

Kuburich, N.A., Kiselka, J.M., den Hollander, P., Karam, A.A., Mani, S.A., 2024. The cancer chimera: impact of vimentin and cytokeratin Co-Expression in hybrid Epithelial/Mesenchymal cancer cells on tumor plasticity and metastasis. Cancers 16, 4158. https://doi.org/10.3390/cancers16244158.

Kwan, R., Chen, L., Looi, K., Tao, G.-Z., Weerasinghe, S.V., Snider, N.T., Conti, M.A., Adelstein, R.S., Xie, Q., Omary, M.B., 2015. PKC412 normalizes mutation-related keratin filament disruption and hepatic injury in mice by promoting keratin-myosin binding. Hepatol. Baltim. Md 62, 1858–1869. https://doi.org/10.1002/hep.27965.

Laly, A.C., Sliogeryte, K., Pundel, O.J., Ross, R., Keeling, M.C., Avisetti, D., Waseem, A., Gavara, N., Connelly, J.T., 2021. The keratin network of intermediate filaments regulates keratinocyte rigidity sensing and nuclear mechanotransduction. Sci. Adv. 7, eabd6187. https://doi.org/10.1126/sciadv.abd6187.

Latorre, E., Kale, S., Casares, L., Gómez-González, M., Uroz, M., Valon, L., Nair, R.V., Garreta, E., Montserrat, N., Del Campo, A., Ladoux, B., Arroyo, M., Trepat, X., 2018. Active superelasticity in three-dimensional epithelia of controlled shape. Nature 563, 203–208. https://doi.org/10.1038/s41586-018-0671-4.

Lehmann, S.M., Leube, R.E., Windoffer, R., 2021. Growth, lifetime, directional movement and myosin-dependent motility of mutant keratin granules in cultured cells. Sci. Rep. 11, 2379. https://doi.org/10.1038/s41598-021-81542-8.

Lim, H.Y.G., Alvarez, Y.D., Gasnier, M., Wang, Y., Tetlak, P., Bissiere, S., Wang, H., Biro, M., Plachta, N., 2020. Keratins are asymmetrically inherited fate determinants in the mammalian embryo. Nature 585, 404–409. https://doi.org/10.1038/s41586-020-2647-4.

Lim, H.Y.G., Plachta, N., 2021. Cytoskeletal control of early mammalian development. Nat. Rev. Mol. Cell Biol. 22, 548–562. https://doi.org/10.1038/s41580-021-00363-9.

Lorenz, C., Köster, S., 2022. Multiscale architecture: mechanics of composite cytoskeletal networks. Biophys. Rev. 3, 031304. https://doi.org/10.1063/5.0099405.

Lu, H., Hesse, M., Peters, B., Magin, T.M., 2005. Type II keratins precede type I keratins during early embryonic development. Eur. J. Cell Biol. 84, 709–718. https://doi.org/10.1016/j.ejcb.2005.04.001.

Marikawa, Y., Alarcon, V.B., 2018. RHOA activity in expanding blastocysts is essential to regulate HIPPO-YAP signaling and to maintain the trophectoderm-specific gene expression program in a ROCK/actin filament-independent manner. Mol. Hum. Reprod. 25, 43–60. https://doi.org/10.1093/molehr/gay048.

Moch, M., Herberich, G., Aach, T., Leube, R.E., Windoffer, R., 2013. Measuring the regulation of keratin filament network dynamics. Proc. Natl. Acad. Sci. 110, 10664–10669. https://doi.org/10.1073/pnas.1306020110.

Moch, M., Leube, R.E., 2021. Hemidesmosome-Related keratin filament bundling and nucleation. Int. J. Mol. Sci. 22, 2130. https://doi.org/10.3390/ijms22042130.

Moch, M., Schwarz, N., Windoffer, R., Leube, R.E., 2020. The keratin–desmosome scaffold: pivotal role of desmosomes for keratin network morphogenesis. Cell. Mol. Life Sci. 77, 543–558. https://doi.org/10.1007/s00018-019-03198-y.

Moll, R., Divo, M., Langbein, L., 2008. The human keratins: biology and pathology. Histochem. Cell Biol. 129, 705–733. https://doi.org/10.1007/s00418-008-0435-6.

Mullins, R.D., Heuser, J.A., Pollard, T.D., 1998. The interaction of Arp2/3 complex with actin: nucleation, high affinity pointed end capping, and formation of branching networks of filaments. Proc. Natl. Acad. Sci. 95, 6181–6186.

Ohsugi, M., Larue, L., Schwarz, H., Kemler, R., 1997. Cell-Junctional and cytoskeletal organization in mouse blastocysts lacking E-Cadherin. Dev. Biol. 185, 261–271. https://doi.org/10.1006/dbio.1997.8560.

Oshima, R.G., Howe, W.E., Klier, F.G., Adamson, E.D., Shevinsky, L.H., 1983. Intermediate filament protein synthesis in preimplantation murine embryos. Dev. Biol. 99, 447–455. https://doi.org/10.1016/0012-1606(83)90294-4.

Outla, Z., Prechova, M., Korelova, K., Gemperle, J., Gregor, M., 2025. Mechanics of cell sheets: plectin as an integrator of cytoskeletal networks. Open Biol. 15, 240208. https://doi.org/10.1098/rsob.240208.

Perrin, L., Matic Vignjevic, D., 2023. The emerging roles of the cytoskeleton in intestinal epithelium homeostasis. Semin. Cell Dev. Biol. Cell Biol. Gut 150–151, 23–27. https://doi.org/10.1016/j.semcdb.2023.03.008.

Pradeau-Phélut, L., Etienne-Manneville, S., 2024. Cytoskeletal crosstalk: a focus on intermediate filaments. Curr. Opin. Cell Biol. 87, 102325. https://doi.org/10.1016/j.ceb.2024.102325.

Prechova, M., Adamova, Z., Schweizer, A.-L., Maninova, M., Bauer, A., Kah, D., Meier-Menches, S.M., Wiche, G., Fabry, B., Gregor, M., 2022. Plectin-mediated cytoskeletal crosstalk controls cell tension and cohesion in epithelial sheets. J. Cell Biol. 221, e202105146. https://doi.org/10.1083/jcb.202105146.

Pruyne, D., Evangelista, M., Yang, C., Bi, E., Zigmond, S., Bretscher, A., Boone, C., 2002. Role of formins in actin assembly: nucleation and Barbed-End association. Science 297, 612–615. https://doi.org/10.1126/science.1072309.

Quinlan, R.A., Schwarz, N., Windoffer, R., Richardson, C., Hawkins, T., Broussard, J.A., Green, K.J., Leube, R.E., 2017. A rim-and-spoke hypothesis to explain the biomechanical roles for cytoplasmic intermediate filament networks. J. Cell Sci. 130, 3437–3445. https://doi.org/10.1242/jcs.202168.

Rawe, V.Y., Payne, C., Schatten, G., 2006. Profilin and actin-related proteins regulate microfilament dynamics during early mammalian embryogenesis. Hum. Reprod. 21, 1143–1153. https://doi.org/10.1093/humrep/dei480.

Schwarz, N., Leube, R.E., Düsterhöft, S., 2025. Comprehensive in silico analyses of keratin heterodimerisation. Eur. J. Cell Biol. 104 (4), 151513. https://doi.org/10.1016/j.ejcb.2025.151513.

Schwarz, N., Moch, M., Windoffer, R., Leube, R.E., 2016. Multidimensional monitoring of keratin intermediate filaments in cultured cells and tissues. Methods Enzym. 568, 59–83. https://doi.org/10.1016/bs.mie.2015.07.034.

Schwarz, N., Windoffer, R., Magin, T.M., Leube, R.E., 2015. Dissection of keratin network formation, turnover and reorganization in living murine embryos. Sci. Rep. 5. https://doi.org/10.1038/srep09007.

Slager, H.G., Good, M.J., Schaart, G., Groenewoud, J.S., Mummery, C.L., 1992. Organization of non-muscle myosin during early murine embryonic differentiation. Differentiation 50, 47–56. https://doi.org/10.1111/j.1432-0436.1992.tb00485.x.

Spector, I., Shochet, N.R., Blasberger, D., Kashman, Y., 1989. Latrunculins—novel marine macrolides that disrupt microfilament organization and affect cell growth: I. Comparison with cytochalasin d. Cell Motil. 13, 127–144. https://doi.org/10.1002/cm.970130302.

Sun, S.-C., Wang, Q.-L., Gao, W.-W., Xu, Y.-N., Liu, H.-L., Cui, X.-S., Kim, N.-H., 2013. Actin nucleator Arp2/3 complex is essential for mouse preimplantation embryo development. Reprod. Fertil. Dev. 25, 617–623. https://doi.org/10.1071/RD12011.

Tateishi, K., Nishida, T., Inoue, K., Tsukita, S., 2017. Three-dimensional organization of layered apical cytoskeletal networks associated with mouse airway tissue development. Sci. Rep. 7, 43783. https://doi.org/10.1038/srep43783.

Toivola, D.M., Boor, P., Alam, C., Strnad, P., 2015. Keratins in health and disease. Curr. Opin. Cell Biol. 32, 73–81. https://doi.org/10.1016/j.ceb.2014.12.008.

Toivola, D.M., Goldman, R.D., Garrod, D.R., Eriksson, J.E., 1997. Protein phosphatases maintain the organization and structural interactions of hepatic keratin intermediate filaments. J. Cell Sci. 110, 23–33. https://doi.org/10.1242/jcs.110.1.23.

Wang, F., Chen, S., Liu, H.B., Parent, C.A., Coulombe, P.A., 2018. Keratin 6 regulates collective keratinocyte migration by altering cell-cell and cell-matrix adhesion. J. Cell Biol. 217, 4314–4330. https://doi.org/10.1083/jcb.201712130.

Windoffer, R., Leube, R.E., 1999. Detection of cytokeratin dynamics by time-lapse fluorescence microscopy in living cells. J. Cell Sci. 112, 4521–4534.

Wolf, K.M., Mullins, J.M., 1987. Cytochalasin B-induced redistribution of cytokeratin filaments in PtK1 cells. Cell Motil. Cytoskelet. 7, 347–360. https://doi.org/10.1002/cm.970070407.

Wöll, S., Windoffer, R., Leube, R.E., 2005. Dissection of keratin dynamics: different contributions of the actin and microtubule systems. Eur. J. Cell Biol. 84, 311–328. https://doi.org/10.1016/j.ejcb.2004.12.004.

Yamamura, S., Goda, N., Akizawa, H., Kohri, N., Balboula, A.Z., Kobayashi, K., Bai, H., Takahashi, M., Kawahara, M., 2020. Yes-associated protein 1 translocation through actin cytoskeleton organization in trophectoderm cells. Dev. Biol. 468, 14–25. https://doi.org/10.1016/j.ydbio.2020.09.004.

Yoon, K.H., Yoon, M., Moir, R.D., Khuon, S., Flitney, F.W., Goldman, R.D., 2001. Insights into the dynamic properties of keratin intermediate filaments in living epithelial cells. J. Cell Biol. 153, 503–516. https://doi.org/10.1083/jcb.153.3.503.

Zenker, J., White, M.D., Gasnier, M., Alvarez, Y.D., Lim, H.Y.G., Bissiere, S., Biro, M., Plachta, N., 2018. Expanding actin rings zipper the mouse embryo for blastocyst formation. Cell 173, 776–791.e17. https://doi.org/10.1016/j.cell.2018.02.035.

Zhu, M., Cornwall-Scoones, J., Wang, P., Handford, C.E., Na, J., Thomson, M., Zernicka-Goetz, M., 2020. Developmental clock and mechanism of de novo polarization of the mouse embryo. Science 370, eabd2703. https://doi.org/10.1126/science.abd2703.